Simulating the Nonlinear Dynamics of the VTOL System

Jordan Thuo[1], n11046252

***Abstract*— This report presents the development and implementation of a control system for the AV-8A Harrier, focusing on achieving stable hover and precise landing. The control system design employs both state-feedback and output-feedback strategies, with a Linear Quadratic Regulator (LQR) for optimal state-feedback control. Iterative refinement and gain scheduling were utilized to enhance controller performance, ensuring a smooth descent and minimizing overshoot. The state observer accurately estimates unmeasured states, crucial for output-feedback control. Simulations conducted using MATLAB and Simulink demonstrate the effectiveness of the control system in managing the complex dynamics of the AV-8A Harrier, with significant improvements in stability and control precision. The findings highlight the system's robustness, making it suitable for military and civilian VTOL applications. Future work will explore further enhancements, including linear interpolation for gain scheduling, and incorporating a Kalman filter**

I. Introduction

Vertical Take-Off and Landing (VTOL) aircraft, like the AV-8A Harrier, are pivotal advancements in aviation, allowing for vertical take-offs, hovers, and landings. This capability is crucial in military operations where runways may be unavailable. However, controlling VTOL aircraft is complex due to their dynamic behavior and sensitivity to external disturbances, necessitating a robust control system for stability, precision, and safety during flight, especially during hovering and landing.

This report focuses on regulating the Harrier to land smoothly at a zero state/setpoint, ensuring stable hover followed by a controlled descent. The system is modelled as a six-state system in a 2D plane, consisting of: x and y positions, roll angle θ, velocities $\dot{x}$ and $\dot{y}$, and angular velocity $\dot{\theta}$. This simplified model captures the essential dynamics required for control system design.

The primary objective is to design a complete output-feedback control system for the AV-8A Harrier, modeling its dynamics in hover mode to maintain stable position and orientation given arbitrary initial conditions. The report is structured as follows:

[1] System Description and Modelling

[2] State-feedback Control Design

[3] Output-feedback Control Design

[4] Results and Discussion

II. System Description and Modelling

A. Mathematical Model:

The AV-8A Harrier's dynamics can be described by a set of nonlinear differential equations that account for the forces and moments acting on the aircraft. These equations take into account the aircraft's position and orientation (x, y, θ) of the centre of mass. The scaled parameters for this system are sourced from an example from the California University of Technology:

- $m = 4kg$ (mass of the plane)
- $J = 0.0475\ kgm^2$ (moment of inertia)
- $r = 0.25\ m$ (thrust offset)
- $g = 9.8\ m/s^2$ (gravitational constant)
- $c = 0.05\ Ns/m$ (damping coefficient)

The forces generated by the main downward thruster and the manoeuvring thrusters are resolved into a pair of forces F_1 and F_2, acting at a distance r below the aircrafts centre of mass. Evidently, figure (1) illustrates the forces acting on the aircraft.

Figure 1: Front view of simplified vehicle in 2D plane

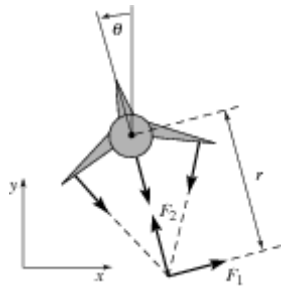

By combining the CCR and SSR, the mathematical model of system can be obtained. The resulting equations of motion for the vehicle are given by:

$$m\ddot{x} = F_1 \cos(\theta) - F_2 \sin(\theta) - c\dot{x} \quad (1)$$

$$m\ddot{y} = F_1 \sin(\theta) + F_2 \cos(\theta) - mg - c\dot{y} \quad (2)$$

$$J\ddot{\theta} = rF_1 \quad (3)$$

These second-order differential equations describe the motion of the vehicle in a 2D plane, capturing the effects of thrust, gravity, and damping on the aircraft's dynamics.

The control inputs for the system can be defined as $u_1 = F_1$ and $u_2 = F_2 - mg$ for the x and y axes, respectively.

[1] **Jordan Thuo** is with Faculty of Engineering, Queensland University of Technology (QUT), Australia. This report is in partial fulfilment of EGH445 unit assessment requirements and **submitted on 19/05/2024.** jordan.thuo@connect.qut.edu.au

Substituting the inputs for the forces in the above equations gives:

$$\ddot{x} = \frac{1}{m}\left(u_1 \cos(\theta) - F_2 \sin(\theta) - c\dot{x}\right) \quad (4)$$

$$\ddot{y} = \frac{1}{m}\left(u_1 \sin(\theta) + (u_2 + mg)\cos(\theta) - mg - c\dot{y}\right) \quad (5)$$

$$\ddot{\theta} = \frac{r}{J} u_1 \quad (6)$$

The state vector z is defined as:

$$z = [x \quad y \quad \theta \quad \dot{x} \quad \dot{y} \quad \dot{\theta}]^T \quad (7)$$

Therefore, the state vector representation of the system dynamics is:

$$\frac{dz}{dt} = \begin{bmatrix} z_4 \\ z_5 \\ z_6 \\ \frac{1}{m}\left(u_1 \cos(z_3) - (u_2 + mg)\sin(z_3) - cz_4\right) \\ \frac{1}{m}\left(u_1 \sin(z_3) + (u_2 + mg)\cos(z_3) - mg - cz_5\right) \\ \frac{r}{J} u_1 \end{bmatrix} \quad (8)$$

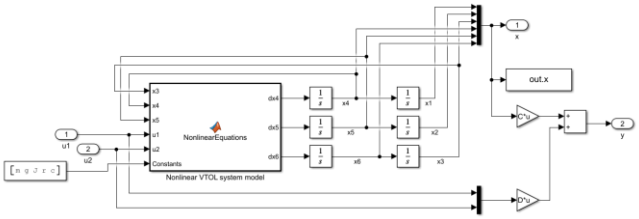

Figure 2: Nonlinear VTOL system model

B. Outputs:

Accurate measurement of specific state variables is essential for the AV-8A Harrier's control system to ensure stable hovering and smooth landing. Initially, measuring roll angle (θ) and the velocities ($\dot{x}$ and $\dot{y}$) was considered, but this configuration lacks observability. If the system is not observable, it is impossible to design an effective observer and controller, leading to potential instability and divergence.

The following sensors are suggested based on cost and reliability:

- Attitude and Heading Reference System (AHRS): Measures the roll angle (θ) using a combination of accelerometers and gyroscopes.[2]
- Global Positioning System (GPS): Provides horizontal position measurements (x).[2]
- Barometric Altimeter: Measures the altitude (y) by sensing air pressure and converting it to altitude based on the standard atmospheric pressure at sea level.[2]

The combination of these three sensors will ensure the system is observable and the output-feedback controller functions effectively. Therefore, the final output matrix C should measure x, y, and θ:

$$C = \begin{bmatrix} 1 & 0 & 0 & 0 & 0 & 0 \\ 0 & 1 & 0 & 0 & 0 & 0 \\ 0 & 0 & 1 & 0 & 0 & 0 \end{bmatrix}$$

C. Linearisation:

Linearising the nonlinear system provides an approximation of the behaviour of the system around an equilibrium point, facilitating the implementation of control strategies such as controllers and observers. This approach simplifies the complex nonlinear dynamics into a linear model that can be effectively analysed and controlled.

However, the linearised model is only accurate near the equilibrium point. Significant deviations can lead to performance issues as the linear model may not capture all nonlinear effects, impacting stability. External disturbances such as wind gusts and sensor noise can also affect control accuracy, highlighting the need for robust design considerations.

1) Calculating the Equilibrium Points:

The equilibrium points are determined by setting the time derivatives of the state variables to zero and solving for the state and input values that satisfy this condition:

$$\dot{z} = f(\bar{z}, \bar{u}) = 0 \quad (9)$$

Assuming small angles ($\theta \approx 0$), the nonlinear state space equation provides:

$$\bar{z} = [x_e \quad y_e \quad 0 \quad 0 \quad 0 \quad 0]^T, \qquad \bar{u} = [0 \quad 0]^T \quad (10,11)$$

Where x_e and y_e can be any real number.

2) Derivation:

Linearising around the equilibrium point involves expanding the nonlinear system equations using a Taylor series and retaining the first-order terms. For the system:

$$\dot{z} = f(z, u) \quad (12)$$

The linearized approximation around the equilibrium point (z_e, u_e) is:

$$\dot{\tilde{z}} = A\tilde{z} + B\tilde{u} \quad (13)$$

Where $\tilde{z} = z - z_e$ and $\tilde{u} = u - u_e$.

The matrices A and B are the Jacobians of f with respect to z and u, evaluated at the equilibrium point.

$$A = \frac{\partial f}{\partial z}\Big|_{z=z_e, u=u_e}, \qquad B = \frac{\partial f}{\partial u}\Big|_{z=z_e, u=u_e} \quad (14,15)$$

The Jacobian matrices for the system are:

$$A = \begin{bmatrix} 0 & 0 & 0 & 1 & 0 & 0 \\ 0 & 0 & 0 & 0 & 1 & 0 \\ 0 & 0 & 0 & 0 & 0 & 1 \\ 0 & 0 & -g & -\frac{c}{m} & 0 & 0 \\ 0 & 0 & 0 & 0 & -\frac{c}{m} & 0 \\ 0 & 0 & 0 & 0 & 0 & 0 \end{bmatrix}, \qquad B = \begin{bmatrix} 0 & 0 \\ 0 & 0 \\ 0 & 0 \\ \frac{1}{m} & 0 \\ 0 & \frac{1}{m} \\ \frac{r}{J} & 0 \end{bmatrix} \quad (16,17)$$

$$C = \begin{bmatrix} 1 & 0 & 0 & 0 & 0 & 0 \\ 0 & 1 & 0 & 0 & 0 & 0 \\ 0 & 0 & 1 & 0 & 0 & 0 \end{bmatrix}, \qquad D = \begin{bmatrix} 0 & 0 \\ 0 & 0 \end{bmatrix} \quad (18,19)$$

The linearized state-space representation is then given by:

$$\dot{z} = Az + Bu, \qquad y = Cz + Du \quad (20,21)$$

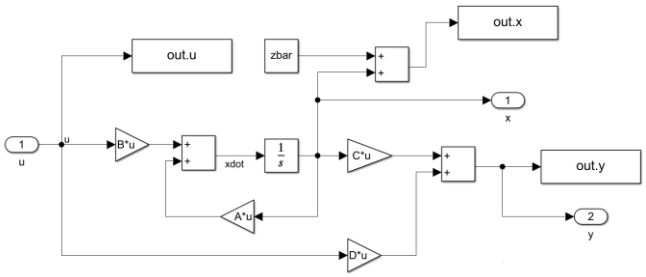

Figure 3: Linearised VTOL system model

The linearised model will provide the foundation for analysing the nonlinear system dynamics. The next section will focus on designing the State-Feedback Controller, to achieve the desired performance objectives for the AV-8A Harrier. This involves determining the appropriate gain matrices to ensure system stability and regulating the aircraft to safely reach its desired state.

III. State-feedback Control Design

A. Open-Loop Stability:

The stability of linearised system can be determined using Lyapunov's First ("Indirect") Method. Considering the nonlinear system linearised about the equilibrium point the eigenvalues of the A matrix are as follows:

$$eig(A) = [0 \quad 0 \quad -0.0125 \quad 0 \quad -0.0125 \quad 0] \quad (22)$$

Since the eigenvalues have repeated zero real parts, system is marginally stable. The presence of zero eigenvalues indicates that the system is not asymptotically stable, but it does not necessarily imply instability.

B. Controllability:

Before a controller can be implemented, the controllability matrix, C_{AB}, should have full rank.

In this case, the controllability matrix is:

$$C_{AB} = [B \quad AB \quad A^2B \quad A^3B \quad A^4B \quad A^5B] \quad (24)$$

Thus, the rank of C_{AB} is:

$$Rank(C_{AB}) = 6 \quad (25)$$

The rank is equivalent to the number of states, suggesting that the linearised system is fully controllable. This is crucial for ensuring that the system can be driven from any initial state to any desired final state within a finite time frame.

C. Set Point Regulation:

To achieve set point regulation, the objective is to design the gain, K, such that the closed-loop system is stable and ensures the system reaches the desired state. The control input into the system can be described as:

$$u = -Kz, \qquad \dot{z} = (A - BK)z \quad (26,27)$$

Implementing negative feedback stabilizes the system and minimizes the error between the current and desired states, z_{ref}:

$$u = -K(z - z_{ref}) \quad (28)$$

This ensures the system moves towards the specified equilibrium points, allowing the aircraft to maintain a stable hover at any x and y position.

D. LQR Tuning and Refinement

The Linear Quadratic Regulator (LQR) optimizes the state-feedback controller by minimizing a cost function:

$$J(z_0, u) = \int_0^\infty (z^T Q z + u^T R u)\, dt \quad (29)$$

$$Q_1 = diag([0.7, 0.5, 1, 1, 1.3, 1]), \qquad R_1 = diag([1.2, 1]) \quad (29)$$

Here, Q and R are weight matrices that balance state deviations and control effort. LQR is preferred over arbitrary pole selection due to its robustness and simplicity. The optimal gain matrix K is found by solving the Algebraic Riccati Equation (ARE):

$$A^T S + SA - SBR^{-1}B^T S + Q = 0 \quad (30)$$

The optimal feedback gain is then given by:

$$K = R^{-1}B^T S \quad (31a)$$

$$K_1 = \begin{bmatrix} -0.7638 & 0 & 7.0849 & -1.3843 & 0 & 1.9403 \\ 0 & 0.7071 & 0 & -0 & 2.5881 & 0 \end{bmatrix} \quad (31b)$$

This report explored iterative refinement to optimise the LQR controller, considering performance metrics such as settling time, overshoot, and control effort. However, this process is computationally expensive and time-consuming, as it requires simulating hundreds of combinations of weight gains. To expedite convergence, upper and lower limits were estimated for each parameter in the Q and R matrices, aiming to achieve stable hover and slow, gradual descent. Therefore, faster convergence for the x position and slower convergence for the y position were prioritised. The second LQR used the Q and R values:

$$Q_2 = diag([1, 0.5, 1, 1, 1.5, 1]), \qquad R_2 = diag([0.9, 1]) \quad (31c)$$

E. Gain Scheduling:

To enhance control performance and ensure safe landing, a gain scheduler was implemented. It switches gain values, K and L, when the aircraft reaches the thrust offset height $y = r = 0.25\ m$. This height is significant because it corresponds to the point where the thrust from the downward thrusters has a critical influence on the aircraft's stability and control dynamics.

Upon descending to $y = 0.25\,m$, the gain scheduler increases the y velocity weight gain in the LQR controller, reducing descent speed and minimizing y position overshoot, thus preventing the aircraft from "burrowing" into the ground.

This gain scheduler effectively manages nonlinear dynamics at low altitudes, ensuring stable transitions from descent to hover and landing. However, drastic gain changes can cause model discontinuities and instability, so only minor adjustments were made. Future improvements could use

linear interpolation between gains for smoother transitions.

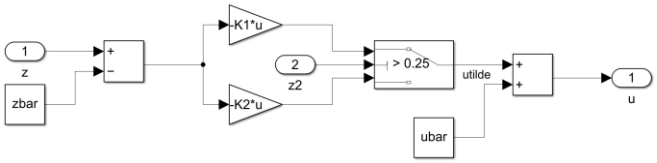

Figure 4: State-feedback Controller

The next section will focus on the Output-Feedback Control Design, where an observer is integrated to estimate the system states based on output measurements, enhancing the robustness and performance of the control system.

IV. Output-Feedback Control

In practical scenarios, it is often not feasible to measure all the states of a system directly. Output-feedback control integrates a state observer to estimate the unmeasured states from the available outputs. The sensors for this system include the AHRS, GPS, and Barometric Altimeter, which measure the roll angle, θ, the x and y positions respectively, to ensure the system is observable. For the AV-8A Harrier, the observability matrix is defined as:

$$O_{CA} = [C \quad CA \quad CA^2 \quad CA^3 \quad CA^4 \quad CA^5]^T \quad (32)$$

Using the output matrix, C, the rank of O_{CA} is six, indicating that the system is observable.

$$Rank(O_{CA}) = 6 \quad (33a)$$

$$L_1 = \begin{bmatrix} 58.2173 & 0 & 0 \\ 0 & 21.5786 & 33.3130 \\ 0 & -12.4098 & 25.5605 \\ 416.8662 & 0 & -9.8000 \\ 0 & 100.5840 & 53.5110 \\ 0 & -5.5722 & 162.3727 \end{bmatrix} \quad (33b)$$

The observer gain matrix L ensures the error dynamics of the Full-order Leunberger Observer converge to zero. The observer equation is given by:

$$\dot{\hat{z}} = A\hat{z} + Bu + L(y - C\hat{z}) \quad (34)$$

Where $\hat{z}$ is the estimated state vector. The error dynamics can be expressed as:

$$\dot{e} = (A - LC)e \quad (35)$$

Where $e = z - \hat{z}$ is the estimation error. The poles of the observer are placed 10 times faster than the closed-loop system poles, following the separation principle for independent observer and controller design, assuming faster observer dynamics.

Although designed for a linearized model, the observer may not fully capture nonlinear behaviour for large deviations. Additionally, placing observer poles significantly faster than closed-loop poles can increase sensitivity to noise and disturbances, leading to inaccurate state estimations and potential instability.

Fast convergence of the observer ensures accurate state estimates, allowing the state-feedback controller to maintain stability and performance. For system synthesis, the observer's estimated states are split into six channels. The model's output, containing only positional states and roll angle, is concatenated with the estimated velocity states, providing the controller with all necessary information for effective regulation.

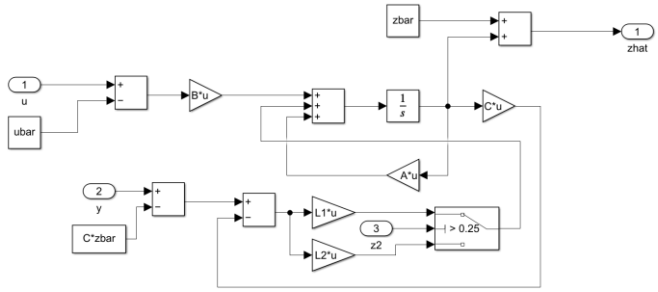

Figure 5: Nonlinear Leunberger Observer

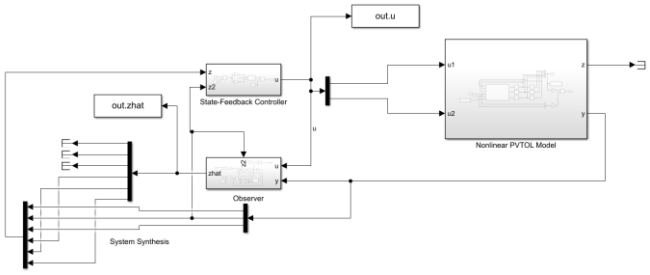

Figure 6: Nonlinear Output-feedback Control System

V. Results and Discussion

To ensure successful convergence, initial conditions were randomly generated:

$$z_0 = [0.7094 \quad 0.7547 \quad 0.2760 \quad 0.6797 \quad 0.6551 \quad 0.1626]^T \quad (36)$$

The equilibrium points are:

$$\bar{z} = [0 \quad 0 \quad 0 \quad 0 \quad 0 \quad 0]^T, \quad \bar{u} = [0 \quad 0]^T \quad (37,38)$$

Simulations were conducted using MATLAB and Simulink with the ODE4 solver for accurate and efficient numerical integration. These simulations provide valuable insights into the performance and limitations of the state-feedback and output-feedback controllers in managing the AV-8A Harrier's dynamics.

A. LQR Closed Loop Response

The state-feedback controller, designed using the Linear Quadratic Regulator (LQR) method, effectively stabilizes the AV-8A Harrier's position and roll angle. Figure 2 shows that both the linear and nonlinear models converge to zero, indicating successful stabilization, though the nonlinear model exhibits slightly higher initial deviations due to its inherent complexities.

Figure 3 demonstrates the effectiveness of iterative refinement in tuning the Q and R matrices, with faster convergence in the x velocity and a more controlled descent in the y velocity. This iterative approach balances priorities of convergence and minimizes overshoot, optimizing controller performance. The inclusion of a gain scheduler further enhanced the performance by adjusting gain values, minimizing y position overshoot for a stable and controlled

landing.

Figure 4 reveals the control input forces F_1 and F_2 over time. The higher initial peaks in the nonlinear system reflect the greater effort needed to correct initial deviations, but these forces stabilize to equilibrium, indicating well-regulated control inputs by the LQR controller.

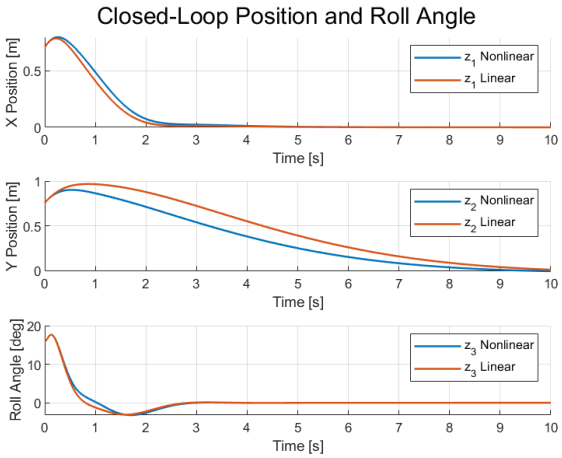

Figure 7: Closed-loop Position and Roll Angle

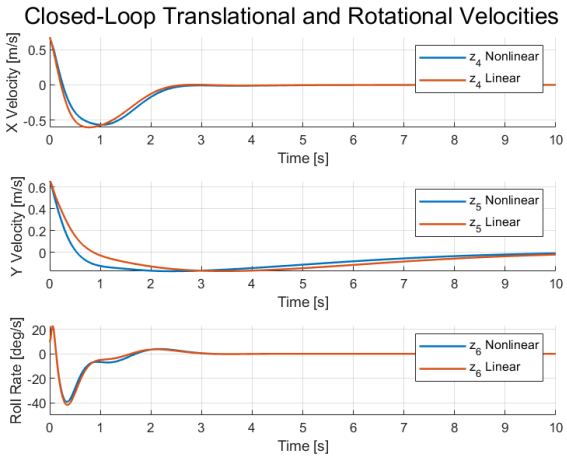

Figure 8: Closed-loop Translational and Rotational Velocities

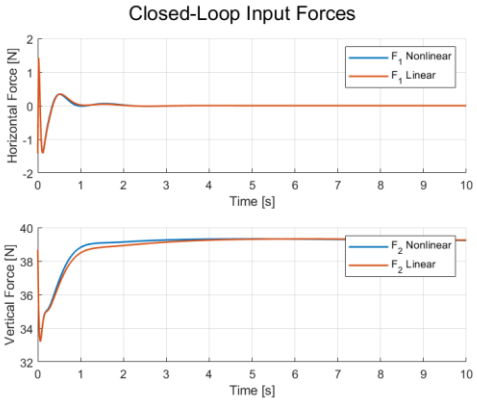

Figure 9: Closed-loop Input Forces

B. *Full Order Luenberger Closed Loop Response:*

Figure 5 demonstrates the observer's accuracy, with close alignment between estimated (dashed lines) and actual states (solid lines), confirming its effectiveness. This accurate state estimation is crucial for the output-feedback controller, which relies on these estimates for appropriate control inputs. The estimates for x, y, and θ converge almost immediately, while in figure 6, the velocities take longer due to system synthesis, where positional states are known, but velocities must be estimated. Although, figure 6 shows precise estimation of translational and rotational velocities. The fast convergence of the observer's error dynamics ensures reliable state information for the controller, enhancing overall system stability and performance.

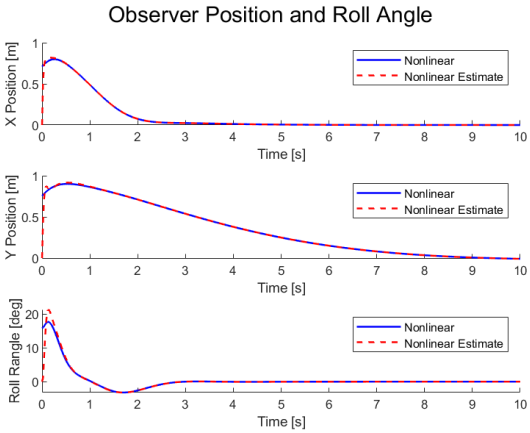

Figure 10: Observer Position and Roll Angle

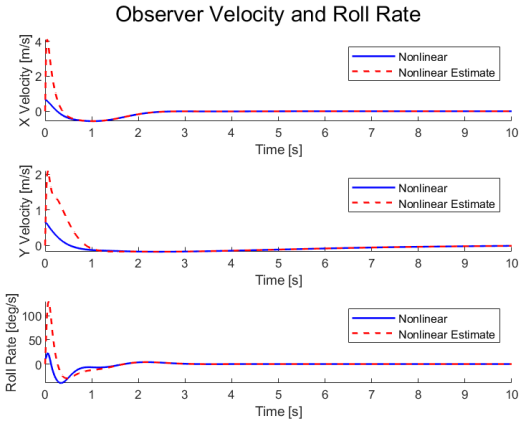

Figure 11: Observer Velocity and Roll Rate

C. *Trajectory and Altitude:*

Figure 7 demonstrates the effectiveness of the gain scheduling strategy and iterative refinement in improving the control system's performance. The optimized gain scheduling LQR controller results in a smoother descent compared to the standard LQR controller. By adjusting the gain at the critical height $y = 0.25\,m$, the system minimizes y-position overshoot, ensuring a stable and controlled landing. Figure 8 further emphasizes this improvement, showing that the

optimized controller achieves a more controlled descent, reducing the likelihood of the aircraft burrowing into the ground. This adjustment highlights the robustness and precision of the control strategy, crucial for safe VTOL operations.

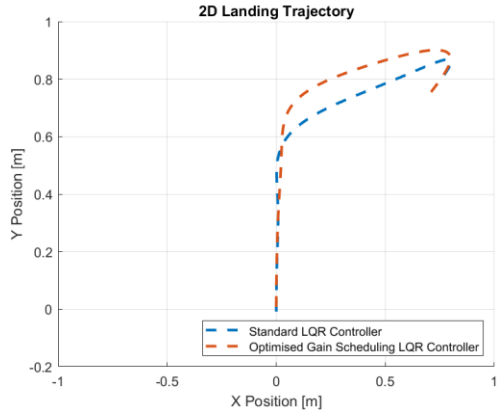

Figure 12: 2D Landing Trajectory

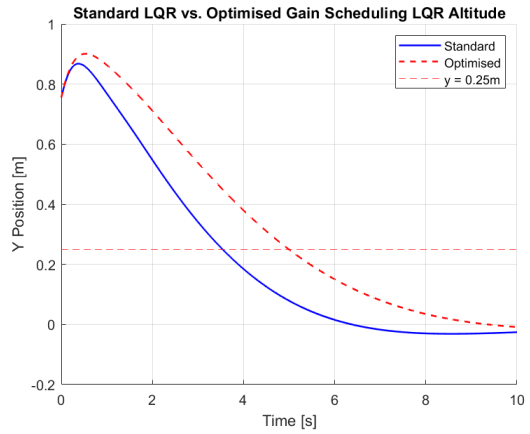

Figure 13: Altitude Heigh Comparison with Optimized LQR

Overall, the analysis of the simulation results demonstrates the successful implementation of the state-feedback and output-feedback controllers. The LQR controller, with iterative refinement and gain scheduling, effectively stabilizes the aircraft's position, velocity, and roll angle, ensuring a smooth and controlled landing. The state observer provides accurate state estimates, enhancing the controller's performance.

VI. Conclusion and Future Work

This report presents the development and implementation of a control system for the AV-8A Harrier, focusing on both state-feedback and output-feedback controllers. The Linear Quadratic Regulator (LQR) combined with a gain scheduler significantly enhances the aircraft's stability during hover and landing. Iterative refinement of the LQR controller ensures an optimal balance between control effort and performance. The gain scheduler manages nonlinear dynamics at critical heights, while the state observer accurately estimates unmeasured states, enabling robust output-feedback control.

The designed controllers ensure stable and precise landing, critical in military operations where runway availability is limited. The robust control design, achieved through iterative refinement and gain scheduling, provides a reliable solution for managing the complex dynamics of VTOL aircraft. This capability also extends to civilian applications, such as urban air mobility, where VTOL aircraft could be used for efficient transportation in congested areas.

A. Potential Improvements and Future Research:

1. **Linear Interpolation for Gain Scheduler**: Smoother transitions between gain values could reduce the risk of discontinuities, enhancing control system robustness during flight phases.
2. **Kalman Filter for State Estimation**: Improved accuracy of state estimation by filtering out sensor noise and disturbances would enhance output-feedback controller performance, especially in the presence of external disturbances.

In conclusion, the control system designed for the AV-8A Harrier represents a significant advancement in VTOL aircraft control. By addressing challenges in nonlinear dynamics and state estimation, the system ensures stable and precise operation. Future research and development efforts focused on these improvements could further enhance VTOL control systems' performance and applicability in both military and civilian domains.

References

[1] Calise, A. J., & Kramer, F. (1982). A Variable Structure Approach to Robust Control of VTOL Aircraft. https://doi.org/10.23919/acc.1982.4788017

[2] Inertial Navigation | TUM – Institute of Flight System Dynamics. (2014). Ed.tum.de. https://www.fsd.ed.tum.de/research/sensors-data-fusion-and-navigation/research-and-competence-areas/inertial-navigation/

[3] Vectored thrust aircraft - FBSwiki. (2024). Caltech.edu. http://www.cds.caltech.edu/~murray/amwiki/Vectored_thrust_aircraft.html#LQR_state_feedback_design

[4] Wikipedia Contributors. (2024, May 6). Harrier jump jet. Wikipedia; Wikimedia Foundation. https://en.wikipedia.org/wiki/Harrier_jump_jet